Shoshonites in Southern Tibet Record Late Jurassic Rifting of a Tethyan Intraoceanic Island Arc

Author(s): J. C. Aitchison, I. R. C. McDermid, J. R. Ali, A. M. Davis, and S. V. Zyabrev

Source: *The Journal of Geology*, Vol. 115, No. 2 (March 2007), pp. 197-213
Published by: The University of Chicago Press
Stable URL: http://www.jstor.org/stable/10.1086/510642

Shoshonites in Southern Tibet Record Late Jurassic Rifting of a Tethyan Intraoceanic Island Arc

J. C. Aitchison, I. R. C. McDermid, J. R. Ali, A. M. Davis, and S. V. Zyabrev[1]

Tibet Research Group, Department of Earth Sciences, University of Hong Kong, Pokfulam Road, Hong Kong Special Administrative Region, China (e-mail: jona@hku.hk)

ABSTRACT

Detailed field mapping combined with a petrologic and geochemical investigation of the Zedong terrane within the Yarlung Tsangpo suture zone provides insights to the evolution of now mostly subducted portions of Tethys during the Late Jurassic. The terrane is dominated by volcanic rocks of shoshonitic affinity, which were erupted in a submarine oceanic island arc setting. The volcanic island arc was built on a basement of oceanic crust, and the shoshonites locally overlie a thin section of pillowed island arc tholeiites and red ribbon–bedded radiolarian cherts. Geochemistry of the shoshonites suggests that their development occurred in a setting analogous to that of Late Miocene to Early Pliocene Fiji and was associated with an arc rifting. We speculate that this event may have been a far-field response to developments associated with Gondwana breakup.

Online enhancements: tables, appendix tables.

Introduction

Potassic igneous rocks are known from a variety of tectonic settings, including within-plate, oceanic (island) arcs, postcollisional arcs, and continental arcs (Müller et al. 1992). They have been reported from numerous locations across the Tibetan Plateau (Arnaud et al. 1992; Turner et al. 1993, 1996; Miller et al. 1999; Williams et al. 2001, 2004; Nomade et al. 2004; Chung et al. 2005). Previously reported rocks are all of continental affinity, and most are Late Cenozoic. Their development has typically been discussed in terms of their significance with respect to the India-Asia collision, the timing of Tibetan Plateau uplift, and the onset on east-west extension of the plateau (Turner et al. 1996; Chung et al. 1998). Other Late Mesozoic examples, however, appear to postdate earlier continental collision events, such as that between the Qiangtang and Lhasa terranes (Pearce and Mei 1988; Chung et al. 1998; Li et al. 2002). We present the first report of shoshonitic series rocks of oceanic affinity from Tibet. The rocks are part of a terrane containing Late Jurassic (Oxfordian to Kimmeridgian) volcanic rocks that is preserved between India and Asia along the Yarlung Tsangpo suture zone (YTSZ). Their development significantly predates any continental collision event and thus provides clues to the history of a now subducted oceanic basin. It is one of the few occurrences where an oceanic island arc origin can be clearly demonstrated for ancient shoshonitic rocks.

Manuscript received December 20, 2005; accepted October 11, 2006.

[1] Present address: Institute of Tectonics and Geophysics, Kim Yu Chen Street, 65, Khabarovsk, 680000 Russia.

Geological Setting

The Zedong terrane (Aitchison et al. 2000; McDermid 2002; McDermid et al. 2002) crops out between the Lhasa and Indian terranes within the YTSZ, which marks the trace of Neotethys. Fragments of one or more ancient submarine volcanic edifices are preserved within the terrane. It is best exposed SE of Lhasa along the southern side of the Yarlung Tsangpo (Yarlung River) either side of the township of Zedong, in Shannan Prefecture (fig. 1). The geology of this area has been mapped in detail (Badengzhu 1979; McDermid 2002), with various aspects having been discussed further by different authors (Yin et al. 1999; Harrison et al. 2000;

[The Journal of Geology, 2007, volume 115, p. 197–213] 0022-1376/2007/11502-0004$15.00

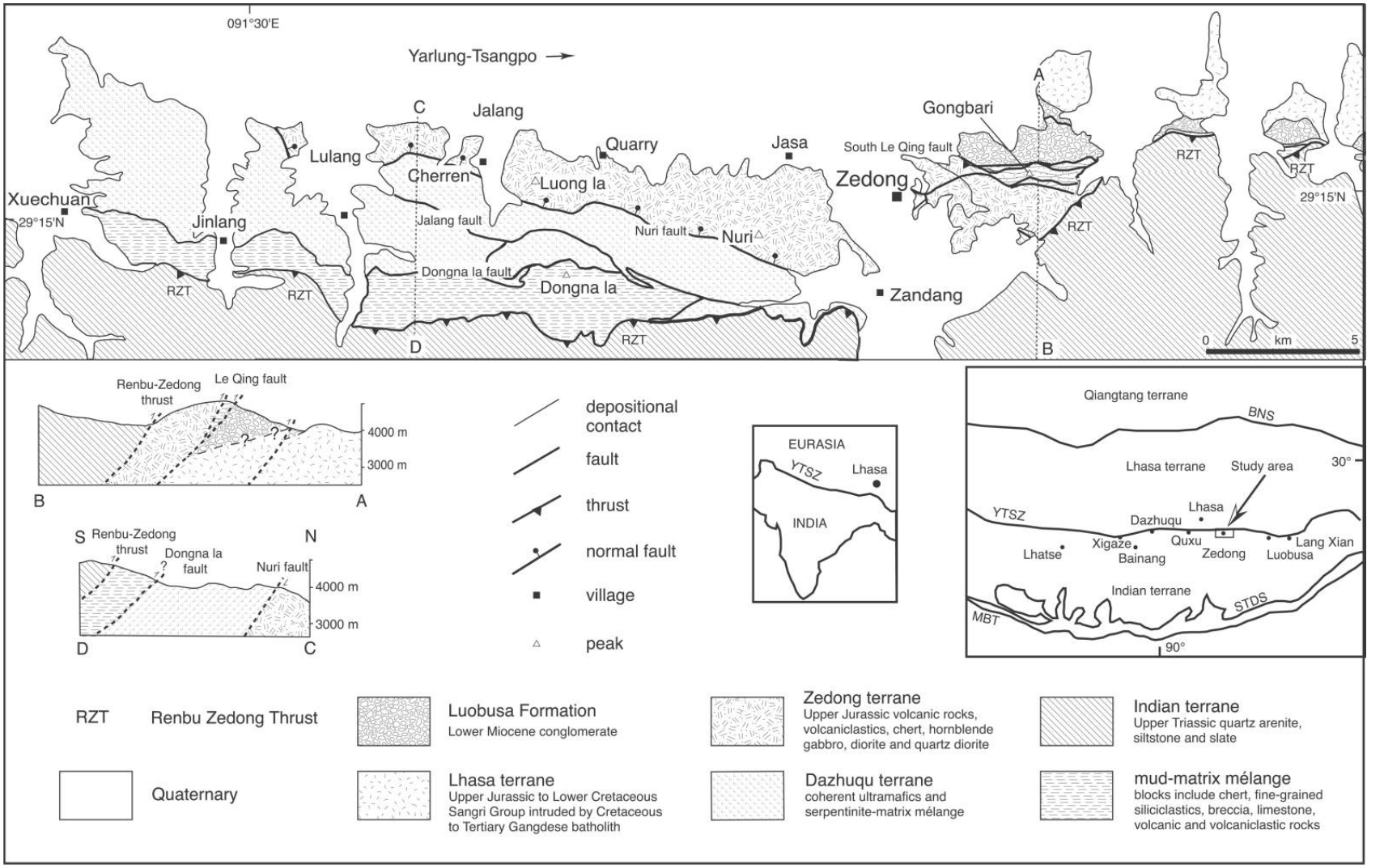

Figure 1. Simplified geological map of the Zedong area (after Badengzhu 1979; McDermid 2002) showing the distribution of rocks assigned to the Zedong terrane. Abbreviations in inset map showing location of study area in Tibet: *MBT* = Main Boundary Thrust; *STDS* = South Tibet Detachment system; *YTSZ* = Yarlung Tsangpo suture zone; *BNS* = Bangong-Nujiang suture.

McDermid 2002; Aitchison et al. 2003). Detailed mapping permits the recognition of a distinctive stratigraphy (McDermid 2002; McDermid et al. 2002) with an overturned succession that includes mostly igneous rocks together with volumetrically subordinate sedimentary lithologies, such as chert, limestone blocks, tuffs, crystal-rich sandstones and mudstones, red siltstones, and volcaniclastic sandstones. Volcanic breccias, most of which are autoclastic, dominate the terrane, and the total preserved stratigraphic thickness locally approaches 1500 m. The terrane is bounded by south-dipping faults. To the north, it is thrust over Lower Miocene Luobusa (Gangrinboche) conglomerates, which unconformably overlie a basement of southern Lhasa terrane rocks (Aitchison et al. 2002, 2003). The southern margin of the terrane is delineated by a steep south-dipping fault along which Zedong terrane rocks lie in the footwall with serpentinized harzburgites in the headwall. This structure is interpreted to have originally been a low-angle normal fault, which together with the entire Zedong terrane stratigraphic succession is now overturned.

Stratigraphy and Petrography

Detailed mapping allows recognition of the former stratigraphic succession within the Zedong terrane (fig. 2). The base of the terrane is faulted with a thin section of tholeiitic plagioclase + olivine + clinopyroxene-phyric pillow basalts (a few tens of meters thick) locally preserved at Luong la, Nuri, Lulang, and near Gongbari. The pillow lavas are overlain by up to 20 m of red ribbon–bedded radiolarian chert. This basal succession indicates that the oldest rocks preserved in the Zedong terrane formed in an oceanic setting. The cherts developed as a result of pelagic sedimentation below the carbonate compensation depth after the cessation of tholeiitic volcanism.

Most of the terrane is, however, dominated by a thick section (up to 1500 m) of autoclastic basaltic volcanic breccias that overlie the tholeiitic basalts and cherts. Basalts and basaltic andesites that typically occur as autoclastic breccias (as well as hyaloclastites) are also locally present as pillow basalts, sheet flows, and dikes. Dacite, rhyolite, and shallow-level subvolcanic intrusions comprise most of the remaining section.

Igneous rocks, including clasts within the breccias that occur stratigraphically above the cherts, are typically porphyritic, with hornblende, plagioclase, and clinopyroxene being the dominant phenocryst phases; olivine and quartz phenocrysts are rare. Volcanic rocks include basalt, basaltic-andesite, dacite, rhyolite, and the shoshonite series equivalents (absarokite, shoshonite, banakite) of these rocks. The breccias are locally intruded by numerous hornblende-phyric, apatite-bearing absarokite dikes, rare dacite dikes, and hornblende gabbro, diorite, and quartz diorite.

Petrographic examination of the autoclastic breccias and dikes permits further discrimination of three types of absarokite on the basis of phenocryst assemblages. Hornblende absarokite is dominated by hornblende with little or no feldspar. Other types of absarokite are dominated by feldspar and clinopyroxene with little or no hornblende or have few phenocrysts. It is likely that some high-K basalts are altered absarokites because they contain microphenocrysts of apatite and bear strong petrographic similarity to the other hornblende absarokites. Hornblende-phyric absarokite lavas are abundant above the lowermost stratigraphic levels in the terrane. Phenocrysts of euhedral to anhedral hornblende, up to 4 mm long, comprise 30%–50% of the total rock volume. Smaller subhedral clinopyroxene phenocrysts are subordinate. Accessory phases include apatite and opaque minerals. Some hornblende phenocrysts have inclusions of clinopyroxene, and crystal margins are locally altered to opaque minerals or chlorite. The groundmass is either microcrystalline or devitrified with glass variably replaced by quartz, epidote, chlorite, and albite. Plagioclase absarokites are dominated by plagioclase phenocrysts set in a pervasively altered groundmass of microcrystalline albite, quartz, and calcite with rare phenocrysts of clinopyroxene, and euhedral hornblende is locally present.

Pillow basalts that occur together with hyaloclastites near Gongbari are, on the basis of stratigraphy, inferred to be younger than those of tholeiitic affinity, which occur at the base of the Zedong terrane. They are shoshonitic and consist of rare (<5% of the total rock volume) variably altered phenocrysts of euhedral plagioclase and subhedral clinopyroxene set in a fine-grained devitrified glassy to microcrystalline groundmass of plagioclase microlaths and rare pyroxene. Calcite locally replaces glomerocrysts, probably of pyroxene. Opaque minerals have cubic, triangular, and hexagonal sections. Irregular and bubble-shaped amygdales filled with secondary minerals, including quartz, prehnite, albite, calcite, epidote, or pumpellyite, account for 10%–30% of the total rock volume. Thin calcite and quartz veins are common.

Hornblende gabbro and diorite form a minor (~10%) component of the terrane intruding the upper portion of the succession. Hornblende exhibits single twins, is rarely zoned, exhibits green to pale

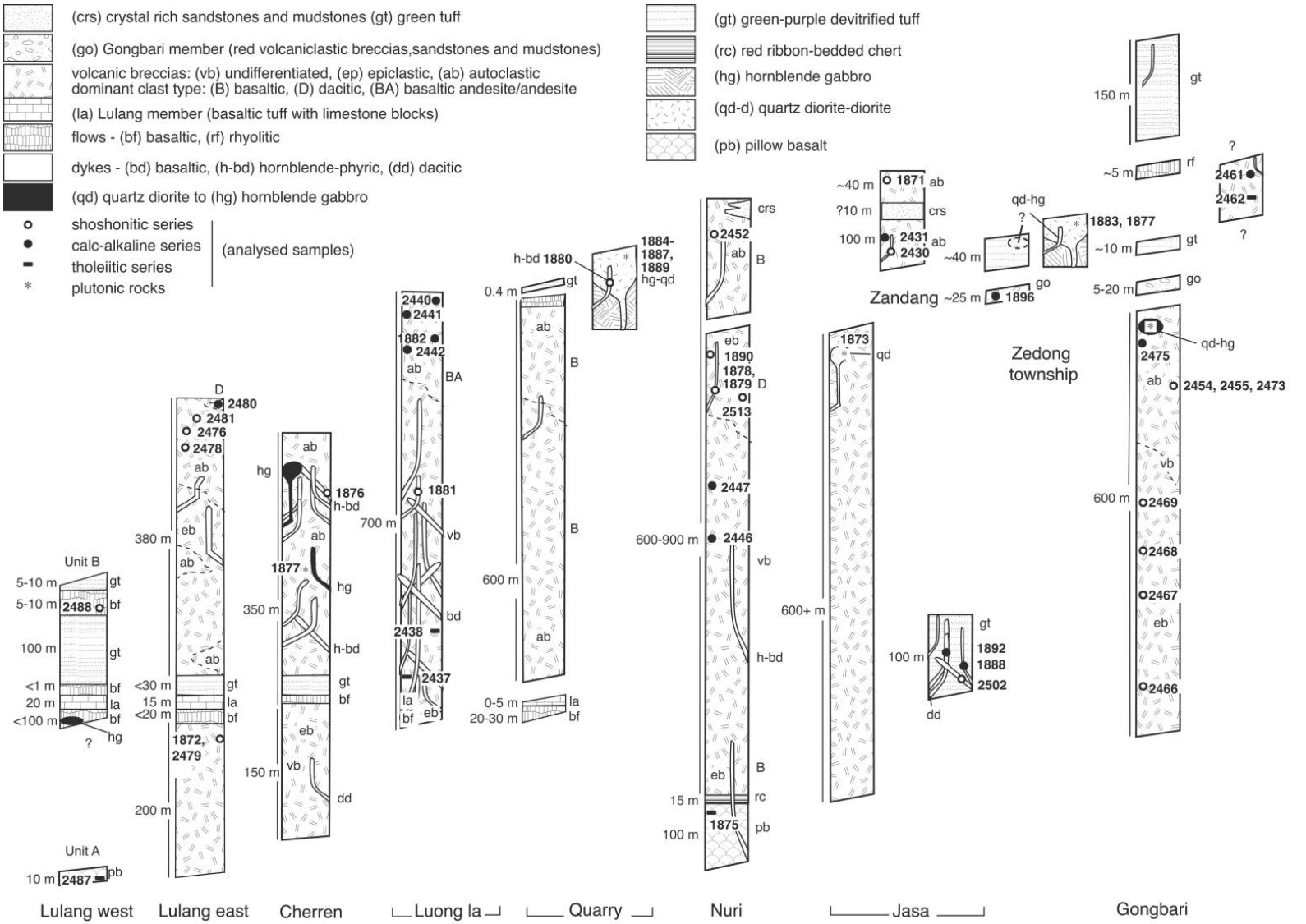

Figure 2. Reconstructed stratigraphic sections compiled from mapping traverses across the Zedong terrane (McDermid 2002), showing the stratigraphic levels from which samples were collected.

green pleochroism, and locally contains small clinopyroxene or plagioclase inclusions. Some are euhedral, whereas other phenocrysts have irregular edges. Secondary minerals include quartz, sericite, chlorite, saussurite, serpentine, epidote, and chlorite. Hornblende gabbros contain 40%–65% hornblende phenocrysts, which enclose plagioclase and clinopyroxene crystals defining a poikilitic texture or fill interstices between euhedral plagioclase. Hornblende is accompanied by plagioclase (35%) and clinopyroxene (1%–5%) phenocrysts with accessory titanite and opaque minerals. Diorites and quartz diorites consist of altered plagioclase and alkali feldspar (55%–70%) hornblende (5%–30%) and quartz (10%–25%) with accessory green biotite, zircon, apatite, titanite, and opaque minerals. Their textures range from anhedral granular to subhedral granular. Rare hornblende crystals are enclosed by quartz in quartz diorite samples. Elsewhere, rare megacrysts of hornblende up to 10 cm long are present.

Although uncommon, porphyritic dacites and rhyolites occur among the breccias in the uppermost part of the terrane. Phenocrysts (0.5–3.0 mm) are moderately abundant to rare and include euhedral to anhedral feldspar (5%–30% of the total rock volume), subhedral hornblende (1%–20%), minor quartz (<5%), and rare clinopyroxene. Feldspar is variably altered and is commonly sericitized. Hornblende margins are altered to chlorite or opaque Fe oxides.

Other lithologies that are present in minor quantities include sedimentary rocks deposited during periods of relative vent quiescence. Carbonate occurs as limestone blocks in the fine-grained tuffs and is interpreted to have accumulated in shallow marine areas during vent quiescence. The blocks may have been dislodged and then redeposited together with ash during renewed tectonic activity associated with the volcanic edifice. Rare monomict volcanic breccias possibly represent resedimented hyaloclastites.

Age

Radiolarian biostratigraphy and geochronology both indicate that the Zedong terrane is late Middle Jurassic–mid Late Jurassic. A well-preserved Bathonian to lower Callovian radiolarian fauna that includes *Stichocapsa robusta* was recovered from near the top (youngest portion) of the red ribbon–bedded chert. This chert overlies the pillowed island arc tholeiite (IAT) lavas and is succeeded by shoshonitic volcaniclastic breccias. *Stichocapsa robusta* constrains the cherts to an interval between the upper Bajocian–lower Bathonian and lower Callovian (Unitary Associations: figs. 5–7 of Baumgartner et al. 1995). The radiolarian fauna thereby constrains the timing of formation of the IAT volcanic rocks and cherts at the base of the terrane to the late Middle Jurassic (McDermid 2002; Ziabrev et al. 2003*a*).

Radiometric dating (laser $^{40}Ar/^{39}Ar$ step heating and U-Pb ion microprobe) of mineral separates from the overlying volcanic pile (McDermid et al. 2002) indicates shoshonitic volcanism occurred in the Late Jurassic between 161 and 152 Ma (Oxfordian to Kimmeridgian), with intrusion of hornblende gabbro and quartz diorites between 163 and 155 Ma. Absarokite dikes intrude these rocks, indicating that shoshonitic magmatism and pluton emplacement were at least partly coeval.

Geochemistry

The geochemistry of 50 rocks from the Zedong terrane was examined (tables 1 and 2 available in the online edition and from the *Journal of Geology* office). Whole-rock samples were taken from the least-altered outcrops and are considered to be representative of the major lithologies in the terrane. Sample locations as recorded by GPS are given in table 1, with the relative stratigraphic positions of samples depicted on reconstructed stratigraphic columns determined from north-south traverses of the terrane (fig. 2). The samples were cut with a diamond-impregnated brass blade, crushed in a steel jaw crusher that was brushed and cleaned with deionized water between samples, and pulverized in agate mortars in order to minimize potential contamination. Major oxides for Zedong terrane rocks (HKU1871-1895) were obtained by wavelength-dispersive X-ray fluorescence spectrometry (WD-XRFS) on fused glass beads using a Philips PW2400 spectrometer at the University of Hong Kong or by inductively coupled plasma atomic emission spectrometry at the Australian Laboratory Services (HKU 1896-2519). Trace elements, including rare earth elements (REEs), were determined by inductively coupled plasma mass spectrometry (ICP-MS) of nebulized solutions using a VG Plasma-Quad Excell ICP-MS at the University of Hong Kong after a 2-d closed beaker digestion using a mixture of HF and HNO_3 acids in high-pressure "bombs" (Qi and Gregoire 2000; Zhou et al. 2004, 2006). Pure elemental standard solutions were used for external calibration, and BHVO-1 and SY-4 were used as reference materials. The accuracies of the XRFS analyses are estimated to be $\pm 2\%$ (relative) for major oxides present in concen-

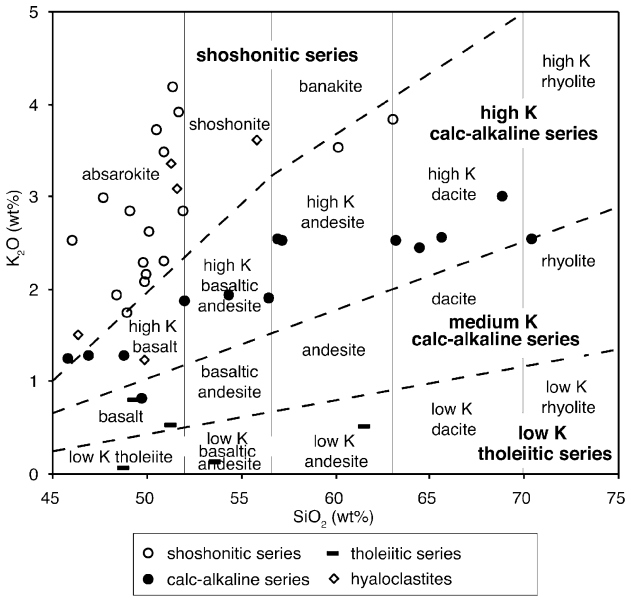

Figure 3. Plot of subalkaline rocks from the Zedong terrane using a K_2O-SiO_2 diagram. The boundaries of absarokite, shoshonite, and banakite follow those of Ewart (1982). All samples are plotted on an anhydrous basis.

trations greater than 0.5 wt% and ±5% (relative) for minor oxides present in concentrations greater than 0.1 wt%. The accuracies of the ICP-MS analyses are estimated to be better than ±5% (relative) for most elements (Zhou et al. 2004).

Aside from rare pillowed tholeiitic basalts locally preserved at the base of the terrane, the Zedong terrane is dominated by a 1500-m section of autoclastic basaltic volcanic breccias. Geochemistry permits discrimination of three broad magmatic associations among this succession: a shoshonitic series, a high-K calc-alkaline series, and a low-K tholeiitic series (fig. 3). The geochemical trend upsection is from tholeiitic at the base of the terrane to shoshonitic in the upper part of the terrane (McDermid 2002).

The pillow basalts at the base of the terrane exhibit trace element and petrographic characteristics of arc tholeiites. The mid-ocean ridge basalt (MORB)–normalized pattern for sample HKU1896 (fig. 4*D*) is enriched in large ion lithophile elements (LILE) and depleted in the high field strength elements (HFSE; Zr, Ti, Hf, Y) and has Nb values <1 typical of oceanic arc tholeiitic series basalts. However, both (Th/Nb)n and (Ce/Nb)n values are >1, which, coupled with the consistent LILE enrichment, suggests that this lava is best classified as an arc tholeiitic basalt.

Shoshonitic Series. Much of Zedong terrane (>45%) is composed of shoshonitic series rocks. Most of these rocks are absarokites (45%–52% SiO_2), with some more evolved shoshonites and banakites (HKU1878, 2513) also present. Major element concentrations for absarokites, aside from K_2O, are similar to those for island arc basalts. They also show a rapid increase in K_2O as silica increases from 45% to 52%. As mentioned earlier, phenocryst assemblages allow the discrimination of hornblende, plagioclase, or pyroxene-phyric absarokites. Shoshonites and banakites are more evolved with higher K_2O and Al_2O_3 and lower MgO, TiO_2, and FeO. They are dominated by feldspar and subordinate clinopyroxene phenocrysts with hornblende as a minor phenocryst phase. The presence of amphibole phenocrysts and accessory apatite indicates that, although altered or devitrified, parent magmas were indeed shoshonitic (Crawford et al. 1992). Two samples (HKU 1872, 2479) with very high K_2O contents (3.82–4.06 wt%), which are markedly more altered than most other samples, are included in the data set in order to provide a representative suite of samples from all stratigraphic levels. They were collected from the lowest breccia horizon in the section on the eastern side of Lulang valley.

Hyaloclastites collected from Gongbari (HKU 2455, 2468, 2469) plot in the high-K calc-alkaline and shoshonitic fields. Other petrographically similar samples (HKU 2467, 2454) are most likely shoshonites from which K has been removed by hydrothermal alteration processes. Alteration of glass to silica-chlorite-albite assemblages is common and often results in partial or extensive depletion of K_2O (Crawford et al. 1992). In all samples, phenocrysts are rare, and plagioclase is now replaced by carbonate. Microphenocrysts of apatite occur as an accessory phase. In comparison with the other absarokites, these sparsely feldspar-phyric samples have lower MgO (~3%) and FeO^* (5%–9%) and higher CaO (8%–13%) and P_2O_5 (0.5%–0.8%) values and are best classified as shoshonites.

Trace element patterns show enrichment in the LILE (Cs, Rb, Ba ≤ 100) and depletion in Nb and Ta relative to the LILE and Ce (fig. 5). The HFSE (Zr, Hf, Ti) and Y are depleted relative to N-MORB. The implications of these shoshonitic series lavas in the Zedong terrane will be considered following presentation of data for the other rocks with which shoshonites are associated.

High-K Calc-Alkaline Series. Fourteen samples plot in this series, including rhyolite, dacites, andesites, basaltic andesites, and basalts, with a few samples plotting below the high-K to medium-K

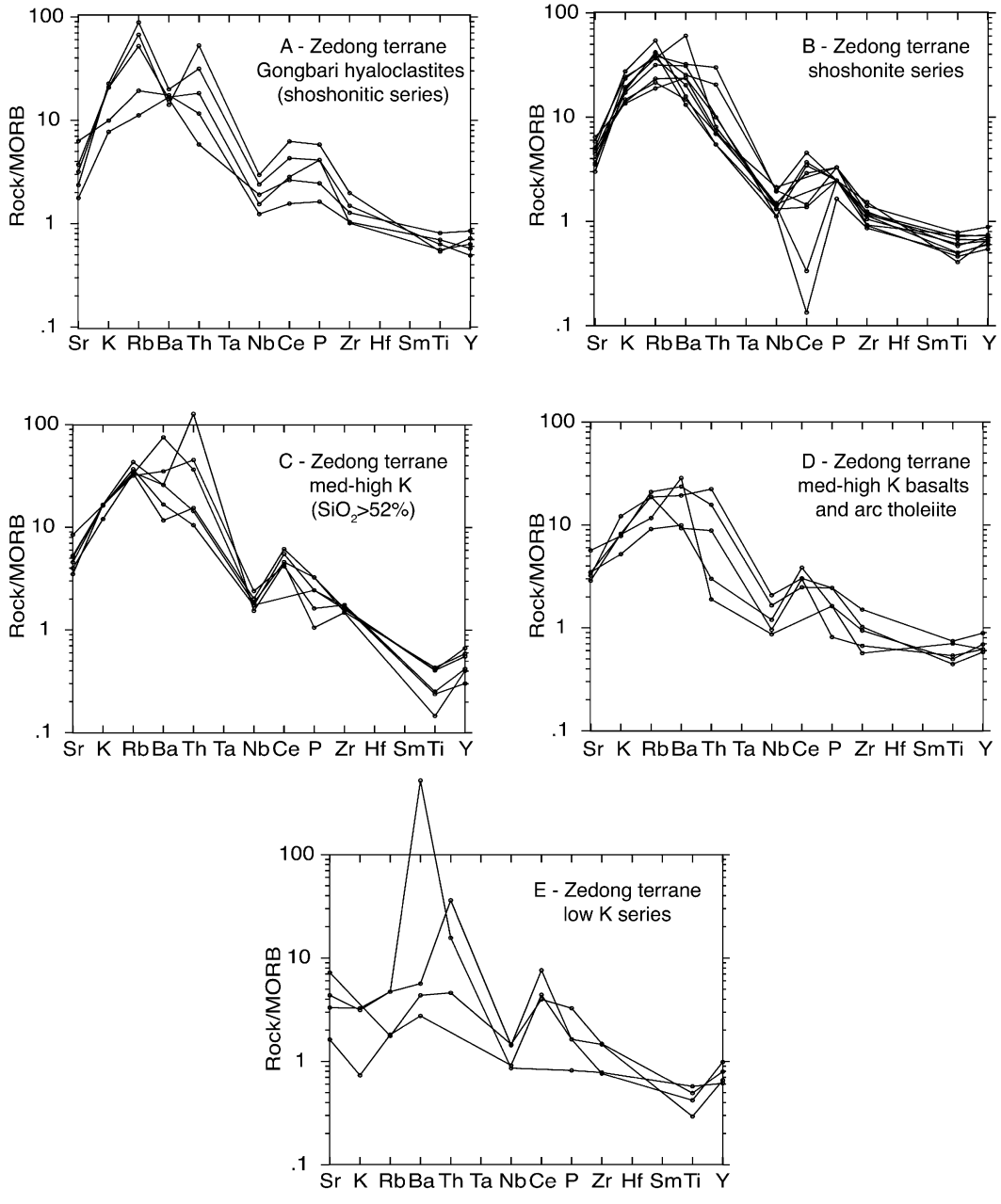

Figure 4. Mid-ocean ridge basalt (MORB)–normalized (Pearce 1982) trace element plots for samples from the Zedong terrane analyzed by X-ray fluorescence (XRF) using pressed pellets. The values for Th and Ce are not plotted for some samples because they were below the detection limit of the XRF.

divide, presumably because of limited K_2O depletion during low-grade metamorphic degradation. High-K basalts have a phenocryst assemblage, which includes plagioclase + hornblende + clinopyroxene ± orthopyroxene ± olivine. Trace element patterns show enrichments in the LILE and depletion in the HFSE (Ti, Y). High-K basaltic andesites and andesites exhibit broadly similar trace element patterns; the LILE are enriched relative to N-MORB, and the HFSE (Ti, Y) are depleted. Zr is slightly enriched relative to MORB, similar to fractionated calc-alkaline rocks. Apart from K_2O, major element concentrations are similar to those for island arc basalts.

Four high-silica samples are also included with the calc-alkaline group. Three (HKU 1888, 1890,

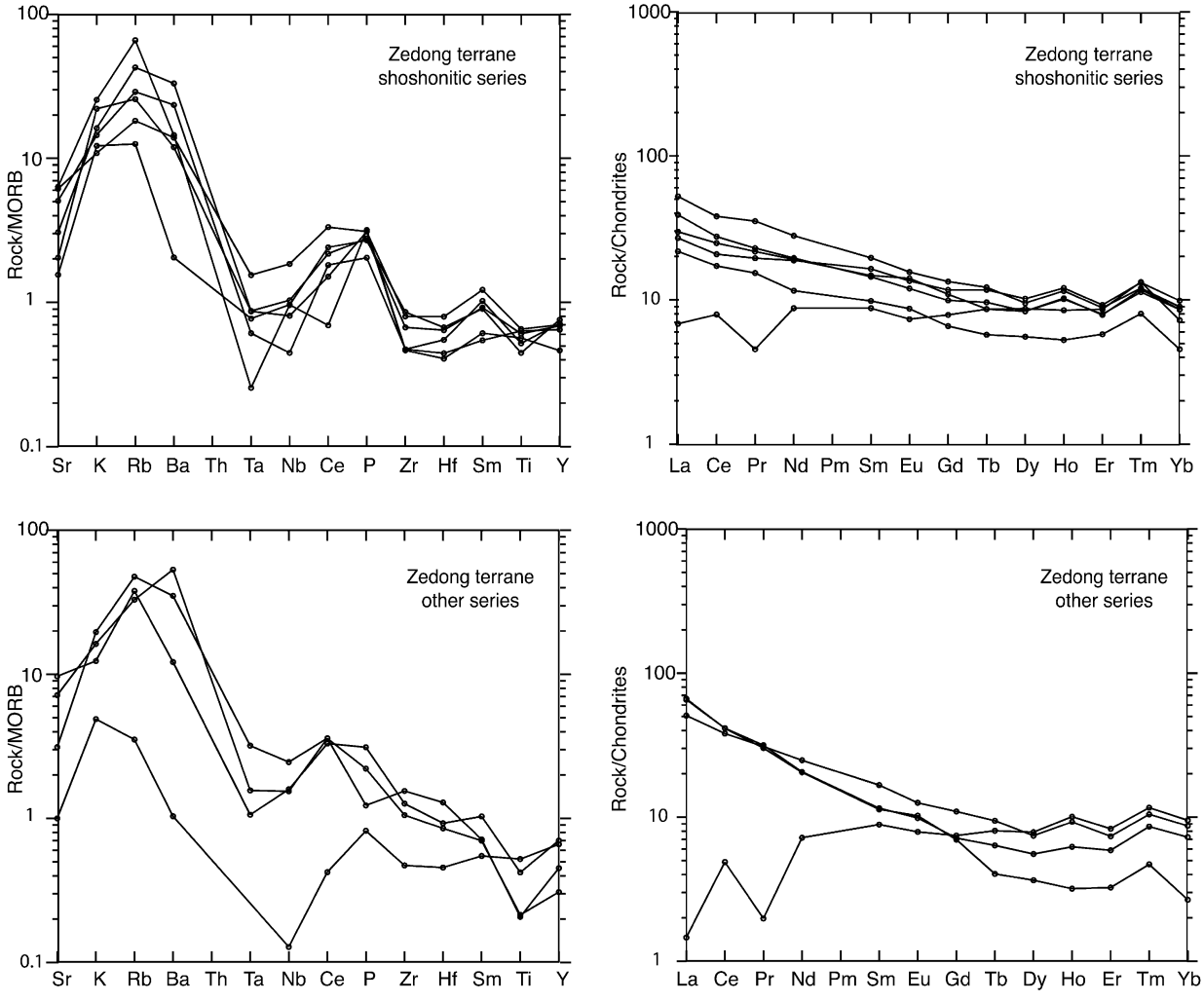

Figure 5. Mid-ocean ridge basalt (MORB)–normalized (Pearce 1982) trace element patterns for samples from the Zedong terrane analyzed by inductively coupled plasma mass spectrometry. Panels show rare earth element patterns (Nakamura 1974).

2480) are dacites. The fourth (HKU 1892) is geochemically a rhyolite, but because the groundmass has been pervasively recrystallized, it is interpreted to have originally been a dacite. The phenocryst assemblage of high silica samples is plagioclase + alkali feldspar + hornblende + clinopyroxene. Apatite was not observed as an accessory phase. Dacites also show enrichment in LILE and depletion in HFSE relative to MORB and are compositionally appropriate for more evolved members of the high-K calc-alkaline suite related by fractionation to the less evolved andesites and basalts in this series.

A single sample (HKU 2446) of medium-K calc-alkaline series affinity from stratigraphically lower in the sequence than most of the shoshonitic series samples is enriched in LILE and Ce and depleted in Nb and the HFSE typical of the calc-alkaline series. It is not as strongly enriched in the LILE and may be interpreted as transitional to the higher-K rocks.

Low-K Calc-Alkaline Series. Three samples (HKU 2437, 2462, 2487) plot in the low-K tholeiitic series, with an additional sample assigned to this group on the basis of petrography and trace element characteristics. Low-K basalts are dominated by clinopyroxene and plagioclase, with hornblende either absent or rare. Trace element patterns are similar to the calc-alkaline series but with consistently lower LILE contents than the high-K series lavas. Two of these low-K calc-alkaline basalts (HKU 2437, 2487) occur low in the stratigraphy, with stratigraphic position of the third sample (HKU

2462) being indeterminate because it was collected from an isolated outcrop.

Interpretation

Most of the Zedong terrane appears to have formed in association with submarine volcanic activity. Volcanic breccias, which dominate the terrane, are remnants of one or more ancient submarine volcanic edifices. They record a drastic change in sedimentation (from radiolarian chert) that occurred with the onset of volcanic activity. Autoclastic breccias formed through the interaction of seawater with coherent lava (quench fragmentation). This process also gave rise to the components of subordinate epiclastic breccias that are interpreted as having been deposited from debris and sediment gravity flows on the flanks of a submarine volcano. It is likely that tectonic activity or gravity acting on unstable slope deposits initiated transportation of these sediments. Stratigraphy and geochemistry indicate that the shoshonitic lithologies, which dominate the terrane, developed over a basement of intraoceanic island arc crust represented by pillowed IAT and chert. Shoshonitic and high-K calc-alkaline rocks are exposed everywhere along strike. Field relations indicate that development of the shoshonitic series rocks was coeval with, and may locally have postdated that of, calc-alkaline series rocks. For example, near Jasa, plagioclase absarokite intrudes high-K dacite dikes, and near Nuri, high-K dacites occur at the same stratigraphic level as shoshonitic dacite (banakite) breccia. A distinct group of shoshonitic hyaloclastites that are sparsely feldspar-phyric and have lower MgO (~3%) and FeO^* (5%–9%) and higher CaO (8%–13%) and P_2O_5 (0.3%–0.8%) values is exposed near Zedong at Gongbari. The shoshonites have distinctive arc trace element patterns, are enriched in LILE, and are depleted in HFSE relative to N-MORB. Thus, they differ considerably from other high-K rocks of continental affinity reported from elsewhere in Tibet.

Shoshonites are not common in oceanic arcs and, where present, have been interpreted (Jakes and White 1972; Morrison 1980; Stern et al. 1988; Gill and Whelan 1989) in various ways, including association with arc maturity, arc continent collision, arc seamount collision, and arc rifting as well as being indicators of depth to the Benioff zone. Of these, an arc continent collision such as that observed in Taiwan (Chung et al. 2001) can be ruled out because geochemistry, sedimentology, and the age of the Zedong terrane preclude its development in this setting. The HFSE are noticeably more strongly depleted than those in shoshonitic rocks associated with arc continent collision. Calc-alkaline subduction-related volcanism occurred along the southern margin of Eurasia (Lhasa terrane) from the Late Jurassic to Early Cenozoic, but clastic units of the Zedong terrane lack any continental detritus that might indicate proximity of the arc to a continent. If an island arc had collided with Eurasia, any associated shoshonitic rocks would be more likely to occur within the southern Lhasa terrane. Had the Zedong terrane accreted to the southern margin of Eurasia, it would also have been intruded by Late Cretaceous to Early Cenozoic magmas associated with the Gangdese batholith.

Settings in which shoshonitic volcanic rocks are associated with intraoceanic arc rifting appear to provide more likely analogs for the Zedong terrane succession. The Izu-Bonin-Marianas (IBM) system is a 2500-km-long arc system where the Pacific plate is subducting beneath the Philippine Sea plate. Shoshonitic magmas erupt along a 150-km segment adjacent to the magmatic front in the Northern Seamount Province (Stern et al. 1988; Bloomer et al. 1989) in an area referred to as the Alkalic Volcano Province (AVP). Generation of these rocks has been variously interpreted to be associated with arc rifting following collision of an oceanic plateau (the Ogasawara Plateau; Stern et al. 1984; Honza and Tamaki 1985), development of a new arc segment following arc rifting (Stern et al. 1988), or along strike extension of the arc/forearc region as plate convergence becomes more oblique (Fryer et al. 1997).

Shoshonites in the AVP co-occur with high-K calc-alkaline volcanic rocks. They all are fractionated with moderate to low MgO, Ni, and Cr contents. They are unusual among IBM arc lavas because they are significantly enriched in LILE relative to normal MORB and exhibit LILE and HFSE fractionation more similar to that associated with convergent margin magmas (Sun and Stern 2001). However, relative to continental shoshonites, the LILE and HFSE are depleted (fig. 6). Stern et al. (1988) proposed that the AVP represented a new arc segment built following rifting of an older arc to form the Mariana trough back-arc basin. In this model, the Mariana Trough spreading center is propagating northward through the volcano arc. Young arc volcanoes are expected where a back-arc basin has recently formed because rifting ends the previous cycle of arc magmatism and a new arc begins on the trenchward flank of the rift (Karig 1971; Hawkins et al. 1984). Stern et al. (1988) also used isotopic evidence to argue that the generation of shoshonitic rocks reflects melting of unusually

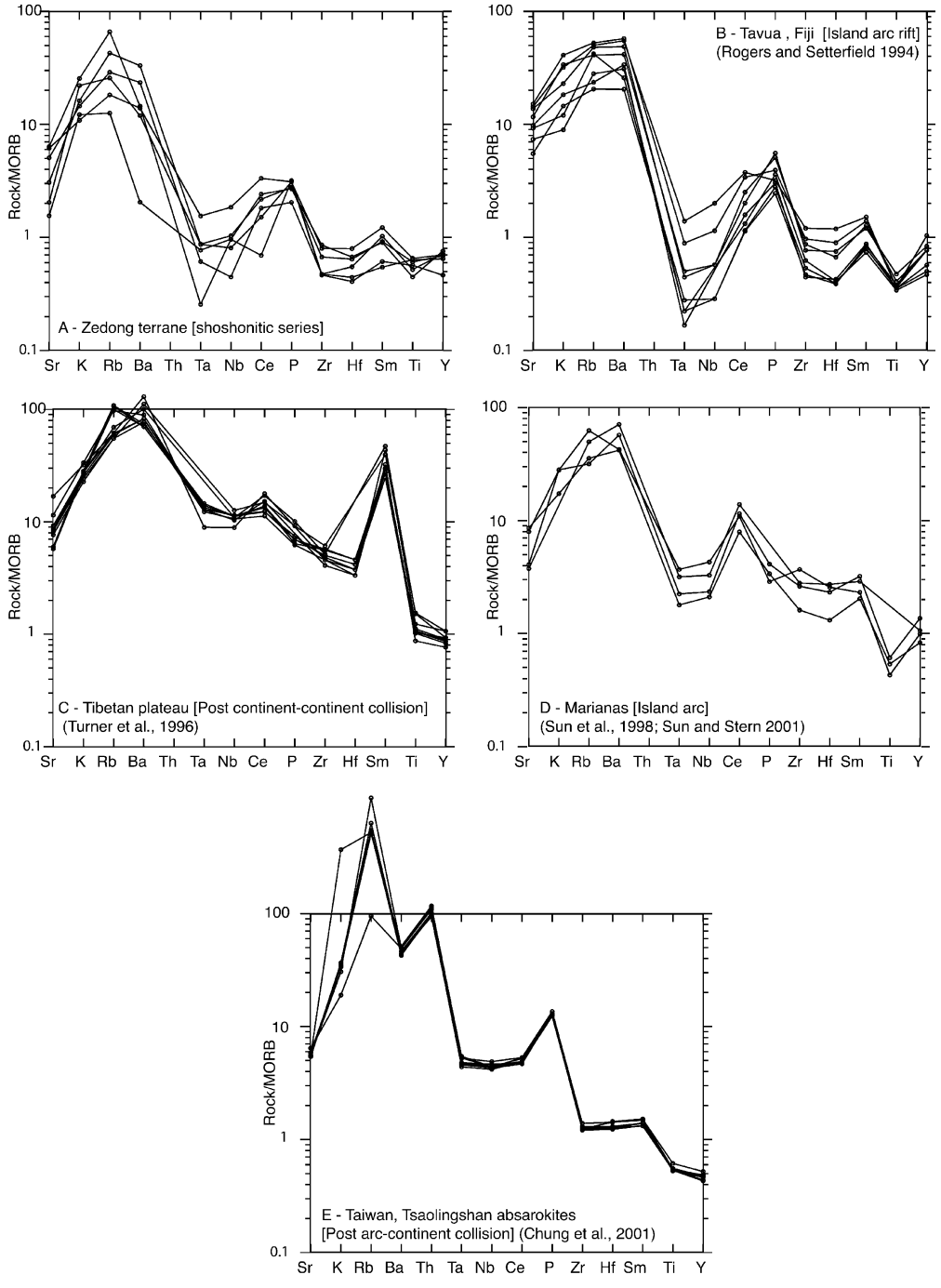

Figure 6. Mid-ocean ridge basalt (MORB)–normalized trace element patterns for shoshonitic series rocks from the Zedong terrane (*A*) compared with those for shoshonites from modern postcollisional (*C*, *E*) and arc settings (*B*, *D*).

enriched parts of the subjacent mantle wedge, a consequence of the interaction between the propagating back-arc rift and the mantle source of arc magmas. The key point is that shoshonite series lavas occur in a restricted section of the arc system in the vicinity of the propagating tip of the Mariana Trough back-arc basin spreading center. The same relatively shallow lithosphere in the upper plate has probably been sampled by partial melting beneath the shoshonitic volcanoes of the southern

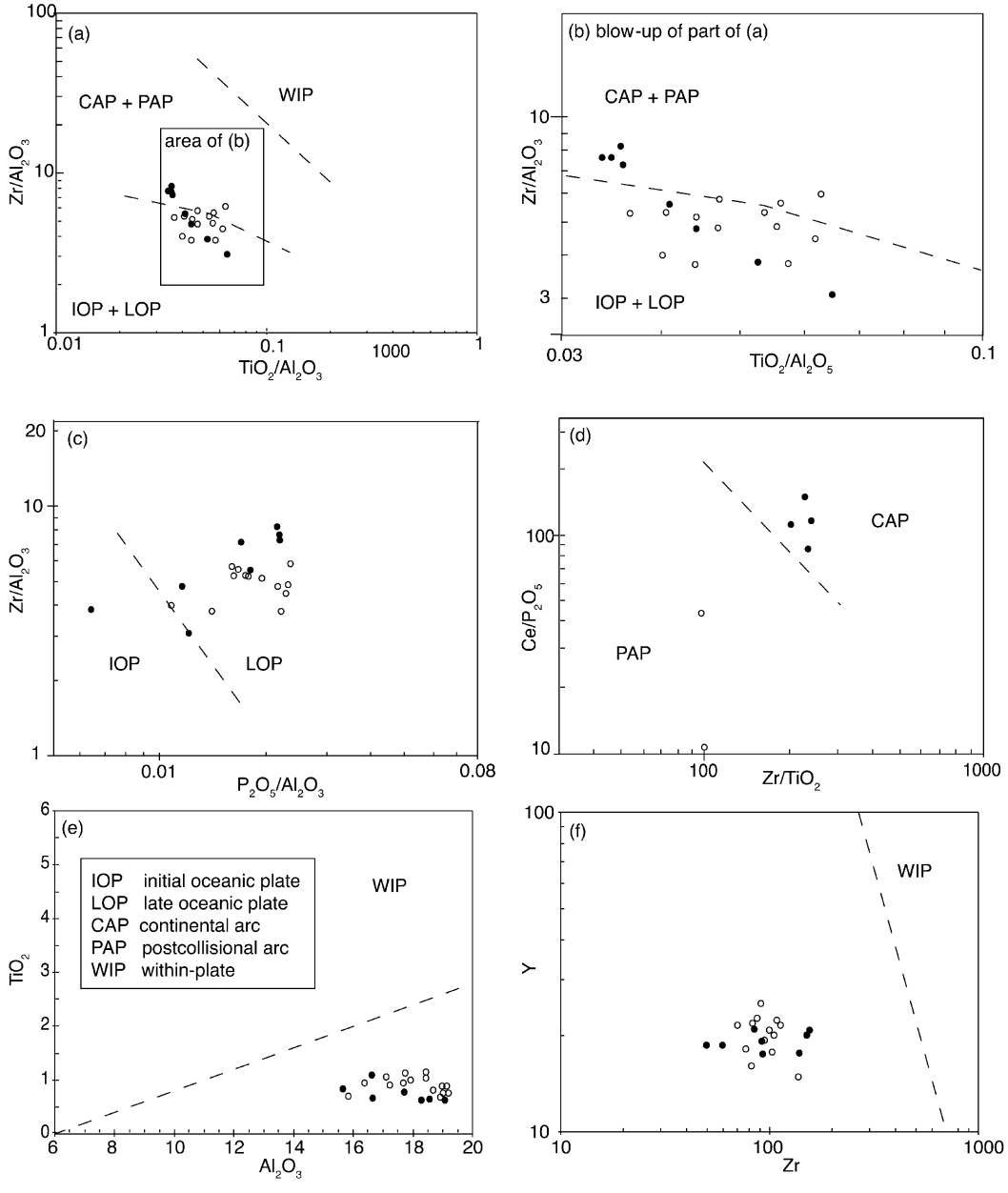

Figure 7. Zedong terrane sample data plotted on discrimination diagrams for potassic igneous rocks from different tectonic settings based on simple ratios of immobile elements. Fields after Müller et al. (1992).

Kasuga cross chain volcanic belt that cuts across the northern portion of the Mariana arc from the trench axis to 60 km west of the magmatic front (Fryer et al. 1997). These volcanoes range in composition from basaltic to dacitic, but both these and the AVP shoshonites are significantly less LILE enriched than the Zedong shoshonites at any stage of fractionation (Stern et al. 1988; Fryer et al. 1997; Sun et al. 1998; Sun and Stern 2001).

In the Fijian islands, Pliocene shoshonitic magmas are associated with fragmentation of the northeast-facing Vitiaz island arc. This arc is situated on the northeast margin of the Indo-Australian plate under which the Pacific plate is being subducted. Before rifting in the Pliocene, the Vitiaz arc was composed of the now separated Lau and Vanautu ridges. The Lau ridge is the remnant arc of the now active Tonga Ridge. The formation of the back-arc basins that separate Fiji from the active subduction sites began during the late Miocene and early Pli-

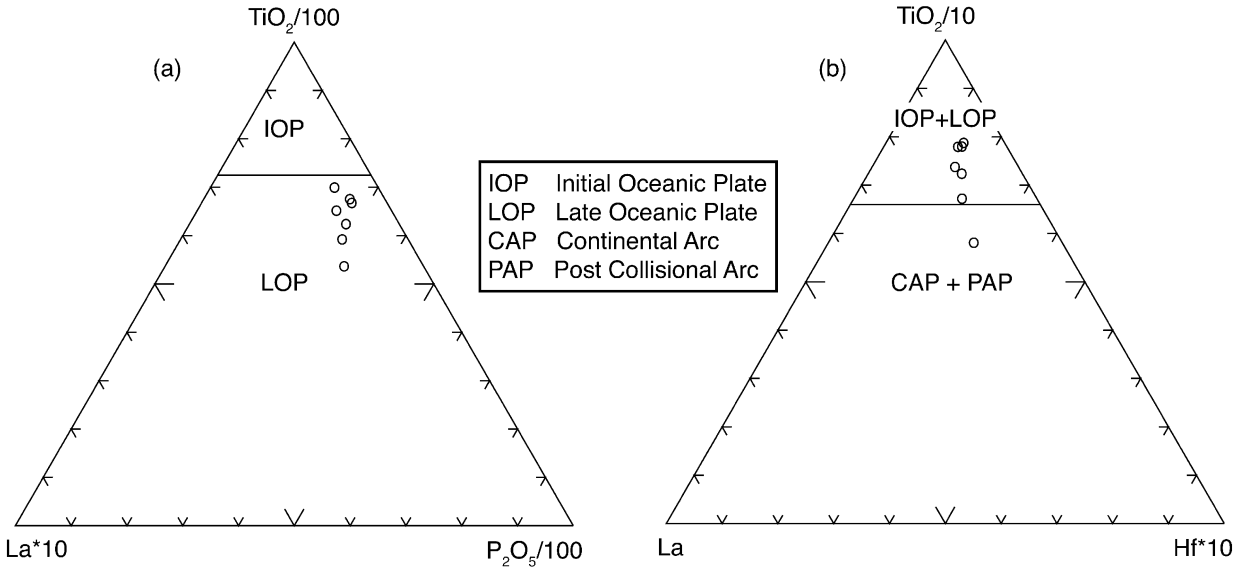

Figure 8. Zedong terrane sample data plotted on ternary trace element discrimination diagrams for potassic igneous rocks. Fields and sample screening criteria after Müller et al. (1992).

ocene (Gill 1984; Gill and Whelan 1989; Rogers and Setterfield 1994; Taylor et al. 2000). Shoshonitic magmatism is interpreted to have begun in Fiji after the formation of a traverse rift that broke the Vitiaz arc across strike. Absarokites were erupted on the remnant arc from 10 volcanoes between 6 and 3 Ma (Gill and Whelan 1989). They were erupted along three lineaments along strike and up to 225 km away from the rift. Medium- and high-K calc-alkaline volcanism was coeval with shoshonitic volcanism. Continued rifting led to the fragmentation of the arc lithosphere and establishment of a back-arc basin spreading center.

Geochemical discrimination diagrams (figs. 7, 8) suggest that the Zedong terrane formed in a late-stage oceanic arc setting analogous to Fiji rather than the AVP in the IBM system, which are erupted along the magmatic front. These diagrams provide a distinction between late-stage and initial island arc settings, but the data for the latter are based on only one modern example (Müller and Groves 2000). Our preferred interpretation is that the shoshonitic volcanism in the Zedong terrane was generated as a result of the rifting of arc lithosphere, as in the case of the Fijian shoshonites.

Discussion

Formation of the Zedong terrane in an intraoceanic setting is consistent with earlier models for development of the YTSZ (Aitchison et al. 2000). However, improved age constraints from radiolarian biostratigraphy and geochronology indicate that it formed largely in the late Middle to mid-Late Jurassic. The occurrence of other intraoceanic supra subduction zone rocks along the YTSZ, such as the mid-Cretaceous ophiolites of the Dazhuqu terrane (Aitchison et al. 2000, 2004; Ziabrev et al. 2003*b*; Dubois-Cote et al. 2005; Dupuis et al. 2005*a*, 2005*b*), and evidence from tomographic imaging for an extensive subducted slab beneath India (Van der Voo et al. 1999) suggest the existence of a long-lived, intraoceanic subduction system within Tethys.

Other evidence of Middle Jurassic to Early Cretaceous intraoceanic subduction is reported from elsewhere along the suture. Ophiolitic rocks of southern Ladakh, including the Spontang, Nidar, and Karzog ophiolites, provide evidence of intraoceanic subduction in the Middle Jurassic and Early Cretaceous. They have supra-subduction zone geochemical signatures and REE patterns that suggest that they may have been broadly cogenetic (Mahéo et al. 2000). Zircons from a plagiogranite in the Spontang ophiolite have yielded a $^{206}Pb/^{235}U$ age of 177 ± 1 Ma (Pedersen et al. 2001). Arc rocks (Spong arc), which overlie the Spontang ophiolite, yield U-Pb ages between 80 and 90 Ma (Pedersen et al. 2001). Further north, the Kohistan Island Arc terrane is interpreted to have evolved over a south-dipping subduction zone through much of Cretaceous time (Dietrich et al. 1983; Schärer et al. 1984; Reuber 1989; Searle et al. 1999). Collision of the

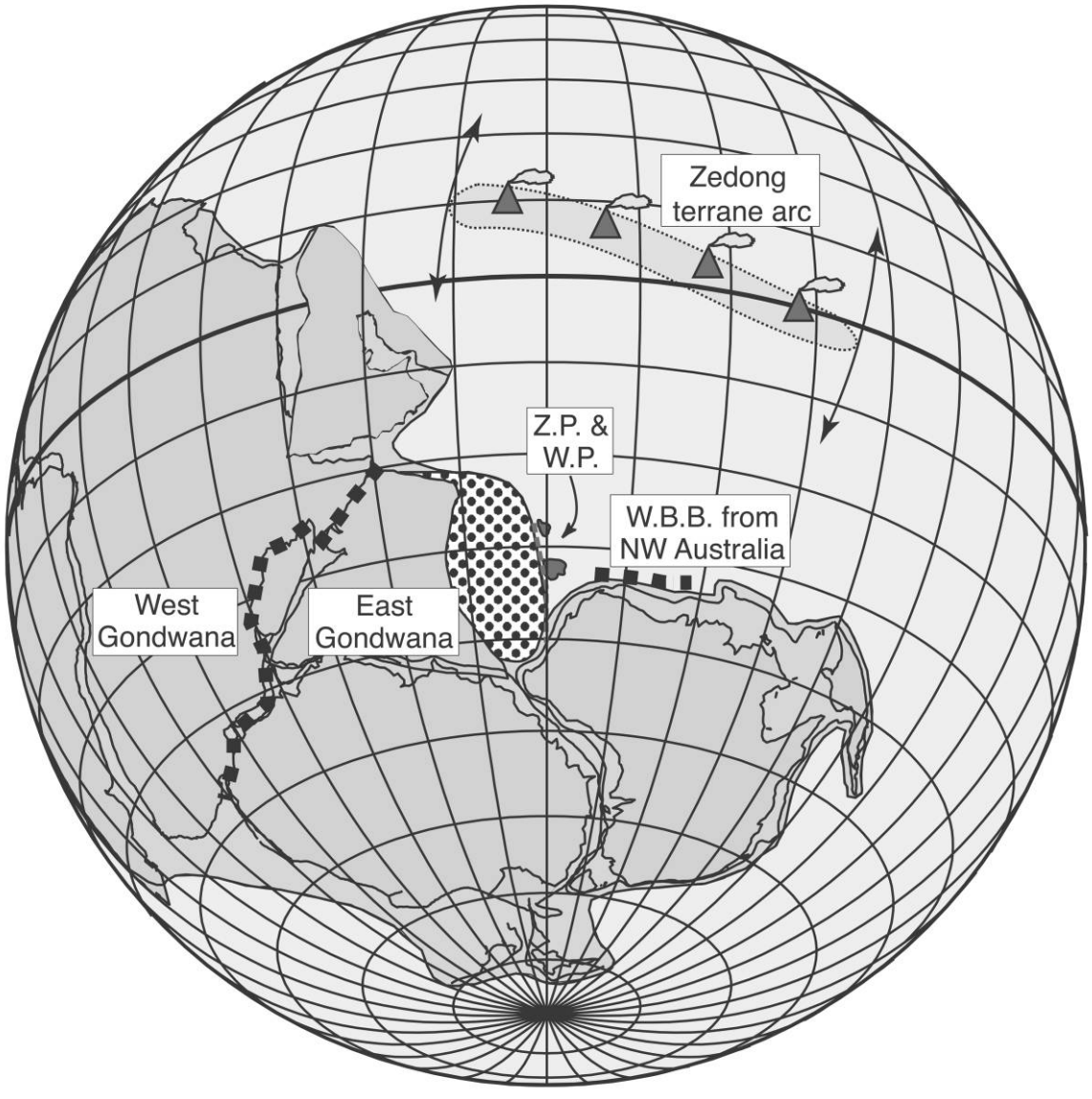

Figure 9. Postulated reconstruction of Gondwana at around 155 Ma. Gondwana stencil from the GMAP program (Torsvik and Smethurst 1999) is positioned using the Besse and Courtillot (2002, 2003) pole for southern Africa; see Ali and Aitchison (2005), particularly concerning "Greater India" (*dotted area*) and the Wallaby (*W.P.*) and Zenith Plateaus (*Z.P.*). Heavy dashed lines represent rifting–early spreading boundaries that started up at about this time for West Burma Block (*W.B.B.*) from NW Australia (Heine et al. 2004) and for West Gondwana from East Gondwana (Schettino and Scotese 2001). Equatorial belt indicates the postulated position in which ophiolitic rocks associated with the Zedong intraoceanic arc may have formed on the basis of the broad equatorial belt in which radiolarian-bearing cherts have tended to form since at least the start of the Mesozoic. We note that this location lies above the 1325-km depth of the high-velocity mantle anomaly III of Van der Voo et al. (1999) interpreted to have been the location of a long-lived zone of intraoceanic subduction with NeoTethys (Abrajevitch et al. 2005).

Kohistan arc with Eurasia to the north caused a new north-dipping subduction zone to form on the south side of this arc, leading to closure of Tethys and India-Asia collision (Robertson and Degnan 1994; Khan et al. 1997). Data presently remain insufficient to resolve whether single or multiple intraoceanic systems are preserved along the suture.

Although a Late Jurassic arc rifting event akin to the Mio-Pliocene event observed in Fiji may have been responsible for development of the Zedong

terrane shoshonites, no other evidence that might imply such an event is known from along the YTSZ. It remains plausible, however, that major events elsewhere in the vicinity or further afield along connected plate margins involved in the development of the Zedong terrane may have resulted in changes in plate motion or poles of rotation that could have triggered arc collapse. In this regard, we note the temporal coincidence of significant events along southern Neotethys during the Kimmeridgian to Oxfordian. Around that time, a fundamental change in plate motions was occurring, with a change from spreading associated with a broadly equatorial Tethys to the development of southwestward-propagating spreading ridges that began to carve up Gondwana. Of potential significance are the Oxfordian rifting of the Argo-Burma terrane from NW Australia (Stampfli and Borel 2002; Heine et al. 2004) and initial separation of Madagascar/Greater India from Africa, which also occurred in the Middle to Late Jurassic (Coffin and Rabinowitz 1987; fig. 9).

In the Paleocene, once the oceanic lithosphere between India and the intra-Tethyan subduction zone was consumed, remnants of the intraoceanic subduction system including Zedong terrane were emplaced onto the Indian margin (Aitchison et al. 2000). Observations from extant intraoceanic arc continent collision zones such as Taiwan and theoretical modeling of such collisions suggest that much of an arc is likely to founder during collision with a continent (Chemenda et al. 2001; Boutelier et al. 2003). Although little of the intraoceanic system is preserved, its collision is clearly recorded along the suture zone in detrital sediments. Coarse-grained clastic sediments derived from the northern India and supra-subduction zone terranes accumulated within the collision zone (Davis et al. 2002) and obduction is heralded by the first arrival ophiolitic detritus shed into latest Paleocene marine sediments on the northernmost margin of India (Ding et al. 2005; Zhu et al. 2005). Ophiolite emplacement was also coincident with the development of widespread melange along the northern margin of India (Liu 2001). By the end of the Paleogene, the Indian Plate, then carrying the extinct intraoceanic arc, collided with the Asian margin (Aitchison et al. 2000; Aitchison and Davis 2004), initiating the Himalayan-Tibet orogeny.

ACKNOWLEDGMENTS

We thank members of the Tibetan Geological Survey (team 2) and the Tibetan Geological Society, especially Badengzhu, whose efforts have helped to make this research possible. Many of our other Tibetan friends have assisted with arranging logistics and permission. F. Xiao and F. Mak are thanked for their assistance with geochemical analysis. We thank S.-L. Chung and A. J. Crawford for their helpful reviews of the manuscript. This work was supported by grants from the Research Grants Council of the Hong Kong Special Administrative Region, China (projects HKU7102/98P, HKU7299/99P, HKU7069/01P, HKU7001/04, and HKU7002/05). The GMAP plate modeling software developed by T. Torsvik was used to create figure 9.

REFERENCES CITED

Abrajevitch, A.; Ali, J. R.; Aitchison, J. C.; Badengzhu; Davis, A. M.; Liu, J. B.; and Ziabrev, S. V. 2005. Neotethys and the India-Asia collision: insights from a palaeomagnetic study of the Dazhuqu ophiolite southern Tibet. Earth Planet. Sci. Lett. 233:87–102.

Aitchison, J. C.; Badengzhu; Davis, A. M.; Liu, J.; Luo, H.; Malpas, J.; McDermid, I.; Wu, H.; Ziabrev, S.; and Zhou, M. F. 2000. Remnants of a Cretaceous intraoceanic subduction system within the Yarlung-Zangbo suture (southern Tibet). Earth Planet. Sci. Lett. 183:231–244.

Aitchison, J. C., and Davis, A. M. 2004. Evidence for the multiphase nature of the India-Asia collision from the Yarlung Tsangpo suture zone, Tibet. *In* Malpas, J. G.; Fletcher, C. J. N.; Ali, J. R.; and Aitchison, J. C., eds. Aspects of the tectonic evolution of China. Geol. Soc. Lond. Spec. Publ. 226:217–233.

Aitchison, J. C.; Davis, A. M.; Ali, J. R.; Badengzhu; Liu, J. B.; Hui, L.; McDermid, I. R. C.; and Ziabrev, S. V. 2004. Stratigraphic and sedimentological constraints on the age and tectonic evolution of the Neotethyan ophiolites along the Yarlung Tsangpo suture zone, Tibet. *In* Dilek, Y., and Robinson, P. T., eds. Ophiolites in earth history. Geol. Soc. Lond. Spec. Publ. 218:147–164.

Aitchison, J. C.; Davis, A. M.; Badengzhu; and Luo, H. 2002. New constraints on the India-Asia collision: the Lower Miocene Gangrinboche conglomerates, Yarlung Tsangpo suture zone, SE Tibet. J. Asian Earth Sci. 21:253–265.

———. 2003. The Gangdese thrust: a phantom structure that did not raise Tibet. Terra Nova 15:155–162.

Ali, J. R., and Aitchison, J. C. 2005. Greater India. Earth-Sci. Rev. 72:169–188.

Arnaud, N. O.; Vidal, P.; Tapponnier, P.; Matte, P.; and Deng, W. M. 1992. The high K_2O volcanism of northwestern Tibet: geochemistry and tectonic implications. Earth Planet. Sci. Lett. 111:351–367.

Badengzhu, comp. 1979. Xizang autonomous region Zhanang: Sangri regional geology reconnaissance map. Xizang Geol. Surv. Geol. Team 2, Lhasa, scale 1 : 50,000.

Baumgartner, P. O.; O'Dogherty, L.; Gorican, S.; Urquhart, E.; Pillevuit, A.; and De Wever, P. 1995. Middle Jurassic to Lower Cretaceous Radiolaria of Tethys: occurrence, systematics, biochronology. Mem. Geol. 23: 1–1172.

Besse, J., and Courtillot, V. 2002. Apparent and true polar wander and the geometry of the geomagnetic field over the last 200 myr. J. Geophys. Res. 107B, doi: 10.029/2000JB000050.

———. 2003. Correction to "Apparent and true polar wander and the geometry of the geomagnetic field over the last 200 myr." J. Geophys. Res. 108B, doi: 10.029/2000JB000050.

Bloomer, S. H.; Stern, R. J.; Fisk, E.; and Geschwind, C. H. 1989. Shoshonitic volcanism in the Northern Mariana Arc. I. Mineralogic and major and trace element characteristics. J. Geophys. Res. 94:4469–4496.

Boutelier, D.; Chemenda, A.; and Burg, J.-P. 2003. Subduction versus accretion of intra-oceanic volcanic arcs: insight from thermo-mechanical analogue experiments. Earth Planet. Sci. Lett. 212:31–45.

Chemenda, A. I.; Yang, R. K.; Stephan, J. F.; Konstantinoskaya, E. A.; and Ivanov, G. M. 2001. New results from physical modelling of arc-continent collision in Taiwan: evolutionary model. Tectonophysics 333: 159–178.

Chung, S.-L.; Chu, M.-F.; Zhang, Y.; Xie, Y.; Lo, C.-H.; Lee, T.-Y.; Lan, C.-Y.; Li, X.; Zhang, Q.; and Wang, Y. 2005. Tibetan tectonic evolution inferred from spatial and temporal variations in post-collisional magmatism. Earth-Sci. Rev. 68:173–196.

Chung, S.-L.; Lo, C. H.; Lee, T. Y.; Zhang, Y. Q.; Xie, Y. W.; Li, X. H.; Wang, K. L.; and Wang, P. L. 1998. Diachronous uplift of the Tibetan plateau starting 40 myr ago. Nature 394:769–773.

Chung, S.-L.; Wang, K.-L.; Crawford, A. J.; Kamenetsky, V. S.; Chen, C.-H.; Lan, C.-Y.; and Chen, C.-H. 2001. High-Mg potassic rocks from Taiwan: implications for the genesis of orogenic potassic lavas. Lithos 59:153–170.

Coffin, M. F., and Rabinowitz, P. D. 1987. Reconstruction of Madagascar and Africa: evidence from the Davie Fracture Zone and Western Somali Basin. J. Geophys. Res. 92:9385–9406.

Crawford, A. J.; Corbett, K. D.; and Everard, J. L. 1992. Geochemistry of the Cambrian volcanic-hosted massive sulfide-rich Mount Read Volcanics, Tasmania, and some tectonic implications. Econ. Geol. 87:597–619.

Davis, A. M.; Aitchison, J. C.; Badengzhu; Luo, H.; and Zyabrev, S. 2002. Paleogene island arc collision-related conglomerates, Yarlung-Tsangpo suture zone, Tibet. Sediment. Geol. 150:247–273.

Dietrich, V.; Frank, W.; and Honegger, K. 1983. A Jurassic-Cretaceous island arc in the Ladakh-Himalayas. J. Volcanol. Geotherm. Res. 18:405–433.

Ding, L.; Kapp, P.; and Wan, X. 2005. Paleocene–Eocene record of ophiolite obduction and initial India-Asia collision, south central Tibet. Tectonics 24:TC3001, doi:10.1029/2004TC001729.

Dubois-Cote, V.; Hebert, R.; Dupuis, C.; Wang, C. S.; Li, Y. L.; and Dostal, J. 2005. Petrological and geochemical evidence for the origin of the Yarlung Zangbo ophiolites, southern Tibet. Chem. Geol. 214:265.

Dupuis, C.; Hebert, R.; Dubois-Cote, V.; Guilmette, C.; Wang, C. S.; Li, Y. L.; and Li, Z. J. 2005*a*. The Yarlung Zangbo Suture Zone ophiolitic melange (southern Tibet): new insights from geochemistry of ultramafic rocks. J. Asian Earth Sci. 25:937–960.

Dupuis, C.; Hebert, R.; Dubois-Cote, V.; Wang, C. S.; Li, Y. L.; and Li, Z. J. 2005*b*. Petrology and geochemistry of mafic rocks from melange and flysch units adjacent to the Yarlung Zangbo Suture Zone, southern Tibet. Chem. Geol. 214:287–308.

Ewart, A. 1982. The mineralogy and petrology of Tertiary–Recent orogenic volcanic rocks: with special reference to the andesite-basalt compositional range. *In* Thorpe, R. S., ed. Andesites. New York, Wiley, p. 25–95.

Fryer, P.; Gill, J. B.; and Jackson, M. C. 1997. Volcanologic and tectonic evolution of the Kasuga seamounts, northern Mariana trough: Alvin submersible investigations. J. Volcanol. Geotherm. Res. 79:277–311.

Gill, J. B. 1984. Sr-Pb-Nd isotopic evidence that both MORB and OIB sources contribute to oceanic island arc magma in Fiji. Earth Planet. Sci. Lett. 68:443–458.

Gill, J. B., and Whelan, P. 1989. Early rifting of an ocean island arc (Fiji) produced shoshonitic to tholeiitic basalts. J. Geophys. Res. 94:4561–4578.

Harrison, T. M.; Yin, A.; Grove, M.; Lovera, O. M.; Ryerson, F. J.; and Zhou, X. 2000. The Zedong Window: a record of superposed Tertiary convergence in southeastern Tibet. J. Geophys. Res. 105:19,211–19,230.

Hawkins, J. W.; Bloomer, S. H.; Evans, C. A.; and Melchior, J. T. 1984. Evolution of intra-oceanic arc-trench systems. Tectonophysics 102:175–205.

Heine, C.; Müller, R. D.; and Gaina, C. 2004. Reconstructing the lost eastern Tethys ocean basin: convergence history of the SE Asian margin and marine gateways. *In* Clift, P. D.; Wang, P.; Khunt, W.; and Hayes, D. E., eds. Continent-ocean interactions within the East Asia marginal seas. Geophys. Monogr. 149:37–54.

Honza, E., and Tamaki, K. 1985. The Bonin arc. *In* Nairn, A. E. M.; Stehli, F. G.; and Uyeda, S., eds. The ocean basins and margins. Vol. 7A. The Pacific Ocean. New York, Plenum, p. 459–502.

Jakes, P., and White, A. J. R. 1972. Major and trace element abundances in volcanic rocks of orogenic areas. Geol. Soc. Am. Bull. 83:29–39.

Karig, D. E. 1971. Origin and development of marginal basins in the western Pacific. J. Geophys. Res. 76: 2542–2561.

Khan, M. A.; Stern, R. J.; Gribble, R. F.; and Windley, B. F. 1997. Geochemical and isotopic constraints on subduction polarity, magma sources and palaeogeography

of the Kohistan intra-oceanic arc, northern Pakistan Himalaya. J. Geol. Soc. Lond. 154:935–946.
Li, X. H.; Zhou, H. W.; Chung, S. L.; Lo, C. H.; Wei, G. J.; Liu, Y.; and Lee, C. Y. 2002. Geochemical and Sr-Nd isotopic characteristics of Late Paleogene ultrapotassic magmatism in southeastern Tibet. Int. Geol. Rev. 44:557–574.
Liu, J. B. 2001. Yamdrok Melange, Gyantze district, Xizang (Tibet), China. MA thesis, University of Hong Kong.
Mahéo, G.; Bertrand, H.; Guillot, S.; Mascle, G.; Pecher, A.; Picard, C.; and De, S. J. 2000. Evidence of a Tethyan immature arc within the South Ladakh ophiolites (NW Himalaya, India). C. R. Acad. Sci. Ser. II A Sci. Terre Planetes 330:289–295.
McDermid, I. R. C. 2002. Zedong terrane, south Tibet. PhD thesis, University of Hong Kong.
McDermid, I. R. C.; Aitchison, J. C.; Davis, A. M.; Harrison, T. M.; and Grove, M. 2002. The Zedong terrane: a Late Jurassic intra-oceanic magmatic arc within the Yarlung-Zangbo suture zone, southeastern Tibet. Chem. Geol. 187:267–277.
Miller, C.; Schuster, R.; Klötzli, U.; Frank, W.; and Purtscheller, F. 1999. Post-collisional potassic and ultrapotassic magmatism in SW Tibet: geochemical and Sr-Nd-Pb-O isotopic constraints for mantle source characteristics and petrogenesis. J. Petrol. 40:1399–1424.
Morrison, G. W. 1980. Characteristics and tectonic setting of the shoshonite rock association. Lithos 13:97–108.
Müller, D., and Groves, D. I. 2000. Potassic igneous rocks and associated gold-copper mineralization. Berlin, Springer.
Müller, D.; Rock, N. M. S.; and Groves, D. I. 1992. Geochemical discrimination between shoshonitic and potassic volcanic rocks in different tectonic settings: a pilot study. Mineral. Petrol. 46:259–289.
Nakamura, N. 1974. Determination of REE, Ba, Fe, Mg, Na and K in carbonaceous and ordinary chondrites. Geochim. Cosmochim. Acta 38:757–775.
Nomade, S.; Renne, P. R.; Mo, X.; Zhao, Z.; and Zhou, S. 2004. Miocene volcanism in the Lhasa block, Tibet: spatial trends and geodynamic implications. Earth Planet. Sci. Lett. 221:227–243.
Pearce, J. A. 1982. Trace element characteristics of lavas from destructive plate margins. *In* Thorpe, R. S., ed. Andesites: orogenic andesites and related rocks. New York, Wiley, p. 525–548.
Pearce, J. A., and Mei, H. 1988. Volcanic rocks of the 1985 Tibet Geotraverse: Lhasa to Golmud. Philos. Trans. R. Soc. Ser. A 327:169–201.
Pedersen, R. B.; Searle, M. P.; and Corfield, R. I. 2001. U-Pb zircon ages from the Spontang Ophiolite, Ladakh Himalaya. J. Geol. Soc. Lond. 158:513–520.
Qi, L., and Gregoire, D. C. 2000. Determination of trace elements in 26 Chinese geochemistry reference materials by inductively coupled plasma mass spectrometry. Geostand. Newsl. 24:51–63.
Reuber, I. 1989. The Dras arc: two successive volcanic events on eroded oceanic crust. Tectonophysics 161: 93–106.
Robertson, A. H. F., and Degnan, P. 1994. The Dras arc complex: lithofacies and reconstruction of a Late Cretaceous oceanic volcanic arc in the Indus suture zone, Ladakh Himalaya. Sediment. Geol. 92:117–145.
Rogers, N. W., and Setterfield, T. N. 1994. Potassium and incompatible-element enrichment in shoshonitic lavas from the Tavua volcano, Fiji. Chem. Geol. 118: 43–62.
Schärer, U.; Rong, H. X.; and Allègre, C. J. 1984. U-Pb geochronology of Gangdese (Transhimalaya) plutonism in the Lhasa-Xigaze region, Tibet. Earth Planet. Sci. Lett. 69:311–320.
Schettino, A., and Scotese, C. R. 2001. New internet software aids paleomagnetic analysis and plate tectonic reconstructions. EOS Trans. Am. Geophys. Union 82:45. http://www.itis-molinari.mi.it/intro-reconstr.html.
Searle, M. P.; Khan, M. A.; Fraser, J. E.; Gough, S. J.; and Jan, M. Q. 1999. The tectonic evolution of the Kohistan-Karakoram collision belt along the Karakoram Highway transect, north Pakistan. Tectonics 18: 929–949.
Stampfli, G. M., and Borel, G. D. 2002. A plate tectonic model for the Paleozoic and Mesozoic constrained by dynamic plate boundaries and restored synthetic oceanic isochrons. Earth Planet. Sci. Lett. 196:17–33.
Stern, R. J.; Bloomer, S. H.; Lin, P.-N.; Ito, E.; and Morris, J. 1988. Shoshonitic magmas in nascent arcs: new evidence from submarine volcanoes in the northern Marianas. Geology 16:426–430.
Stern, R. J.; Smoot, N. C.; and Rubin, M. 1984. Unzipping of the volcano arc, Japan. Tectonophysics 102:153–175.
Sun, C. H., and Stern, R. J. 2001. Genesis of Mariana shoshonites: contribution of the subduction component. J. Geophys. Res. 106:589–608.
Sun, C. H.; Stern, R. J.; Yoshida, T.; and Kimura, J. L. 1998. Fukutoku-oka-no-ba volcano: a new perspective on the Alkalic Volcano Province in the IBM arc. Island Arc 7:432–442.
Taylor, G. K.; Gascoyne, J.; and Colley, H. 2000. Rapid rotation of Fiji: paleomagnetic evidence and tectonic implications. J. Geophys. Res. 105:5771–5781.
Torsvik, T. H., and Smethurst, M. A. 1999. Plate tectonic modelling: virtual reality with GMAP. Comput. Geosci. 25:395–402.
Turner, S.; Arnaud, N.; Liu, J.; Rogers, N.; Hawkesworth, C.; Harris, N.; Kelley, S.; Van Calsteren, P.; and Deng, W. 1996. Post-collision, shoshonitic volcanism on the Tibetan Plateau: implications for convective thinning of the lithosphere and the source of ocean island basalts. J. Petrol. 37:45–71.
Turner, S.; Hawkesworth, C.; Liu, J.; Rogers, N.; Kelley, S.; and Van Calsteren, P. 1993. Timing of Tibetan uplift constrained by analysis of volcanic rocks. Nature 364:50–54.
Van der Voo, R.; Spakman, W.; and Bijwaard, H. 1999. Tethyan subducted slabs under India. Earth Planet. Sci. Lett. 171:7–20.

Williams, H.; Turner, S.; Kelley, S.; and Harris, N. 2001. Age and composition of dikes in southern Tibet: new constraints on the timing of east-west extension and its relationship to postcollisional volcanism. Geology 29:339–342.

Williams, H. M.; Turner, S. P.; Pearce, J. A.; Kelley, S. P.; and Harris, N. B. W. 2004. Nature of the source regions for post-collisional, potassic magmatism in southern and northern Tibet from geochemical variations and inverse trace element modelling. J. Petrol. 45:555–607.

Yin, A.; Harrison, T. M.; Murphy, M. A.; Grove, M.; Nie, S.; Ryerson, F. J.; Wang, X.; and Chen, Z. 1999. Tertiary deformation history of southeastern and southwestern Tibet during the Indo-Asian collision. Geol. Soc. Am. Bull. 111:1644–1664.

Zhou, M.-F.; Ma, Y.; Yan, D.-P.; Xia, X.; Zhao, J.-H.; and Sun, M. 2006. The Yanbian Terrane (Southern Sichuan Province, SW China): a Neoproterozoic arc assemblage in the western margin of the Yangtze Block. Precambrian Res. 144:19–38.

Zhou, M.-F.; Michael Lesher, C.; Yang, Z.; Li, J.; and Sun, M. 2004. Geochemistry and petrogenesis of 270 Ma Ni-Cu-(PGE) sulfide-bearing mafic intrusions in the Huangshan district, Eastern Xinjiang, Northwest China: implications for the tectonic evolution of the Central Asian orogenic belt. Chem. Geol. 209:233–257.

Zhu, B.; Kidd, W. S. F.; Rowley, D. B.; Currie, B. S.; and Shafique, N. 2005. Age of initiation of the India-Asia collision in the East-Central Himalaya. J. Geol. 113: 265–285.

Ziabrev, S.; Aitchison, J. C.; and McDermid, I. 2003*a*. Radiolarian biostratigraphy of the Yarlung-Tsangpo suture, Tibet: a key to understanding the evolution of eastern Tethys. *In* Diserans, M. O., and Jacket, S. J., eds. International Association of Radiolarian Palaeontologists, 10th. Switzerland, University of Lausanne, p. 119.

Ziabrev, S. V.; Aitchison, J. C.; Abrajevitch, A.; Badengzhu; Davis, A. M.; and Luo, H. 2003*b*. Precise radiolarian age constraints on the timing of ophiolite generation and sedimentation in the Dazhuqu terrane, Yarlung-Tsangpo suture zone, Tibet. J. Geol. Soc. Lond. 160:591–600.